Dietary Interaction of High Fat and Marginal Copper Deficiency on Cardiac Contractile Function

David P. Relling, Lucy B. Esberg,* W. Thomas Johnson,† Eric J. Murphy,* Edward C. Carlson,‡ Henry C. Lukaski,† Jack T. Saari,† and Jun Ren**

Abstract

RELLING, DAVID P., LUCY B. ESBERG, W. THOMAS JOHNSON, ERIC J. MURPHY, EDWARD C. CARLSON, HENRY C. LUKASKI, JACK T. SAARI, AND JUN REN. Dietary interaction of high fat and marginal copper deficiency on cardiac contractile function. *Obesity.* 2007; 15:1242–1257.

Objective: High-fat and marginally copper-deficient diets impair heart function, leading to cardiac hypertrophy, increased lipid droplet volume, and compromised contractile function, resembling lipotoxic cardiac dysfunction. However, the combined effect of the two on cardiac function is unknown. This study was designed to examine the interaction between high-fat and marginally copper-deficient diets on cardiomyocyte contractile function.

Research Methods and Procedures: Weanling male rats were fed diets incorporating a low- or high-fat diet (10% or 45% of kcal from fat, respectively) with adequate (6 mg/kg) or marginally deficient (1.5 mg/kg) copper content for 12 weeks. Contractile function was determined with an IonOptix system including peak shortening (PS), time-to-PS, time-to-90% relengthening, maximal velocity of shortening/relengthening, and intracellular Ca^{2+} ($[Ca^{2+}]_I$) rise and decay.

Results: Neither dietary treatment affected blood pressure or glucose levels, although the high-fat diet elicited obesity and glucose intolerance. Both diets depressed PS, maximal velocity of shortening/relengthening, and intracellular Ca^{2+} ($[Ca^{2+}]_I$) rise and prolonged time-to-90% relengthening and Ca^{2+} decay without an additive effect between the two. Ca^{2+} sensitivity, apoptosis, lipid peroxidation, nitrosative damage, tissue ceramide, and triglyceride levels were unaffected by either diet or in combination. Phospholamban (PLB) but not sarco(endo)plasmic reticulum Ca^{2+}-ATPase was increased by both diets. Endothelial NO synthase was depressed with concurrent treatments. The electron transport chain was unaffected, although mitochondrial aconitase activity was inhibited by the high-fat diet.

Discussion: These data suggest that high-fat and marginally copper deficient diets impaired cardiomyocyte contractile function and $[Ca^{2+}]_i$ homeostasis, possibly through a similar mechanism, without obvious lipotoxicity, nitrosative damage, and apoptosis.

Key words: dietary intake, high-fat diet, cardiac dysfunction, copper-deficient diet

Introduction

Uncorrected obesity, a worldwide epidemic problem, is commonly associated with high cardiovascular morbidity and mortality (1–4). Compromised ventricular function occurs in severely obese humans and genetically obese rodents in whole hearts (5,6) and individual cardiomyocytes (7–9). However, the direct impact of obesity on cardiomyocyte function remains poorly defined in the presence of other confounding factors including hypertension, insulin resistance, diabetes, and dyslipidemia (4,7,9–11). Depressed contractile function of cardiomyocytes has been shown in models of genetic obesity with concomitant hypertension (8,9) and diabetes (12,13). Recently, cardiomyocyte contractile dysfunction has also been reported in high-fat diet–induced obesity (14). An increase in tissue triglycerides and

Received for review September 25, 2006.
Accepted in final form November 21, 2006.
The costs of publication of this article were defrayed, in part, by the payment of page charges. This article must, therefore, be hereby marked "advertisement" in accordance with 18 U.S.C. Section 1734 solely to indicate this fact.

*Department of Pharmacology, Physiology, and Therapeutics, University of North Dakota School of Medicine, Grand Forks, North Dakota; †U.S. Department of Agriculture, Agricultural Research Service, Grand Forks Human Nutrition Research Center, Grand Forks, North Dakota; and ‡Department of Anatomy and Cell Biology, University of North Dakota School of Medicine, Grand Forks, North Dakota.
Address correspondence to Jun Ren, Center for Cardiovascular Research and Alternative Medicine, Division of Pharmaceutical Sciences, University of Wyoming, Laramie, WY 82071
E-mail: jren@uwyo.edu

ceramide levels in conjunction with elevation of their circulating levels is perhaps the most detrimental consequence of prolonged high-fat intake and is deemed a hallmark of cardiac lipotoxicity (6,15). Alteration in dietary fatty acid content has a direct impact on body levels of ceramide and triglycerides, which contribute to tissue lipid peroxidation, oxidative and nitrosative damage, and, ultimately, lipotoxicity and cardiac contractile dysfunction (16).

Recent evidence has shown a correlation between coronary vascular risk factors and dietary intake of trace elements including copper, zinc, and selenium in healthy populations (17). The trace element copper is needed for many biological enzymatic processes, including cross-linking of elastin and collagen (lysyl oxidase), synthesis of norepinephrine (dopamine β monooxygenase), and oxidative phosphorylation [cytochrome c oxidase (CCO)].[1] Daily dietary copper intake is usually marginally deficient in most populations (18,19). In addition, convenience foods, which are readily available and high in fat composition, contribute little to the daily dietary requirement for copper ions (19). Therefore, individuals indulging in high fat-containing convenience foods are at great risk for body copper deficiency. More intriguingly, copper deficiency and obesity are intertwined. Genetically obese *ob/ob* mice exhibit lower hepatic copper content despite adequate dietary copper intake (20). In the *fa/fa* obese rats, a primary model of lipotoxic activity, reduced hepatic copper develops (21), which can be overcome by dietary copper supplementation (22). In addition, diabetes, which frequently materializes after sustained obesity, exacerbates tissue copper status (21,23). Reminiscent of data obtained from the genetic *fa/fa* obese rats, high-fat or copper-deficient diet consumption exacerbates copper deficiency-induced cardiomyopathy, a hallmark of copper deficiency (24,25). Copper deficiency-related cardiomyopathy is often manifested by cardiac hypertrophy, depressed contractile function, accumulated lipid deposits, elevated nitric oxide (NO), and apoptosis (19,24,26–28). Interestingly, copper deficiency-induced cardiomyopathy shares some common features with the lipotoxic cardiac dysfunction that originates from hyperlipidemia and accumulation of triglycerides and free fatty acids within cardiomyocytes (6,19). However, whether copper deficiency results in the development of distinctive signs of lipotoxic dysfunction, such as accumulation of ceramide and triglycerides, alteration in NO, and nitrosative damage (6), has not been elucidated. Given that the lipotoxic model (*fa/fa* obese rats) contains reduced tissue copper levels (21,29), the aim of this study was to examine the concurrent impact of high-fat diet and marginal copper deficiency on cardiomyocyte contractile function and intracellular Ca^{2+} $[Ca^{2+}]_i$ handling. Isolated cardiomyocytes offer an immediate assessment of cardiac function independently of fibroblasts and connective tissues, although myocytes may lose the true in vivo physiological environment. To evaluate the potential contribution of lipotoxicity, if any, tissue levels of ceramide, triglycerides, nitrosative damage, apoptosis, electron transport chain (complex I-IV), and mitochondrial aconitase activity were also evaluated in the hearts of rats fed with high-fat and/or marginally copper-deficient diets.

Research Methods and Procedures

Experimental Animals and Diet Feeding

The experimental procedures used in this study were approved by the University of North Dakota and Grand Forks Human Nutrition Research Center (Grand Forks, ND) Animal Use and Care Committees. Weanling male Sprague-Dawley rats weighing 84.5 ± 0.8 grams (Charles River/Sasco, Wilmington, MA) were housed in individual cages in a climate controlled environment (22.8 ± 2 °C, 45% to 50% humidity). Forty animals were randomly assigned, 10 per group, to one of four different experimental diet conditions for 12 weeks of the dietary feeding regimen. The experimental diets were based on the AIN93G diet formulation (Table 1) (30,31). Briefly, the experimental diets included a control diet containing 10% of kilocalories from fat and adequate dietary copper (Cu^{2+}) of 5.0 ± 0.4 mg Cu^{2+}/kg diet (ppm; LFCuA); a high-fat, Cu^{2+}-adequate diet containing 45% of kilocalories from fat and 5.0 ± 0.4 ppm Cu^{2+} (HFCuA); a low-fat, marginally Cu^{2+}-deficient diet containing 10% kilocalories from fat and 1.4 ± 0.1 ppm Cu^{2+} (LFCuD); and a high-fat and marginally Cu^{2+}-deficient diet containing 45% kilocalories from fat and 1.4 ± 0.1 ppm Cu^{2+} (HFCuD; GFHNRC, Grand Forks, ND). Severe copper deficiency (<1.0 mg/kg of diet) was not chosen for our 12-week feeding regimen because of the high incidence of premature death within 5 to 8 weeks of diet feeding. Analysis of dietary copper was obtained from dry ash of a diet sample, by dissolving the ash in aqua regia and measuring the copper quantity through inductive coupled argon photospectrophotometry (ICPP; Model 503; Perkin Elmer, Norwalk, CT). Validation of the assay method was provided by simultaneous assays of reference standards (National Institute of Standards and Technology, Gaithersburg, MD; and Human Nutrition Research Center-2A, Grand Forks, ND, respectively). Body weight (BW), heart rates, systolic blood pressure (BP), and blood glucose levels were assessed reg-

[1] Nonstandard abbreviations: CCO, cytochrome c oxidase; NO, nitric oxide; $[Ca^{2+}]_I$, intracellular Ca^{2+}; LFCuA, low-fat, copper-adequate diet; HFCuA, high-fat, copper-adequate diet; LFCuD, low-fat, marginally Cu^{2+}-deficient diet; HFCuD, high-fat, marginally Cu^{2+}-deficient diet; BW, body weight; BP, blood pressure; FM, fat mass; FFM, fat-free mass; TBIA, tetrapolar bioelectrical impedance analysis; KHB, Krebs-Henseleit bicarbonate; PS, peak shortening; TPS, time-to-PS; TR_{90}, time-to-90% relengthening; ±dL/dt, maximal velocities of shortening/relengthening, maximal slope; SR, sarcoplasmic reticulum; SERCA, sarco(endo)plasmic reticulum Ca^{2+}-ATPase; PLB, phospholamban; eNOS, endothelial NO synthase; STAT, signal transducers and activators of transcription; TLC, thin layer chromatography; TG, triglyceride; GC, gas chromatography; TUNEL, The terminal deoxynucleotidyl transferase-mediated dUTP nick-end labeling; NADH, reduced nicotinamide adenine dinucleotide; SE, standard error.

Table 1. Composition of the experimental diets fed to weanling rats for 12 weeks (grams per kilogram diet)

	LFCuA	LFCuD	HFCuA	HFCuD
High protein casein	189.5	189.6	234.2	234.2
L-cystine	2.8	2.8	3.5	3.5
Sucrose	94.8	94.8	117.1	117.1
Corn starch	450.9	451.7	133.8	134.7
Dyetrose	125.1	125.1	154.6	154.6
Cellulose	47.4	47.4	58.5	58.5
Soybean oil	23.7	23.7	29.3	29.3
Lard	19.9	19.9	212.5	212.5
Choline bitartrate	2.4	2.4	2.9	2.9
Mineral mix	33.2	33.2	41.0	41.0
AIN93G vitamin mix	9.5	9.5	11.7	11.7
Copper premix	0.7	0	0.9	0
Fat content (g/100 g diet)	4.4	4.4	24.2	24.2
Total calories per gram diet	3.9	3.9	4.8	4.8

LFCuA, low-fat, copper-adequate diet; LFCuD, low-fat, marginally Cu^{2+}-deficient diet; HFCuA, high-fat, copper-adequate diet; HFCuD, high-fat, marginally Cu^{2+}-deficient diet.

ularly with a laboratory scale, a semiautomated tail cuff device (IITC, Woodland Hills, CA), and a glucometer (Boehringer Mannheim, Indianapolis, IN), respectively. Initiation of the 12-week feeding regimen was staggered to allow adequate time to perform the cardiomyocyte function study. All chemicals were purchased from Sigma Chemicals (St. Louis, MO) unless otherwise noted.

Tetrapolar Bioelectrical Impedance Analysis

After 11 weeks of dietary feeding, measurements of whole body resistance and whole body reactance were determined to assess fat mass (FM) and fat-free mass (FFM) (32). Briefly, animals were anesthetized with isofluorane, and electrodes were placed. Hypodermic needles (20 gauge; Becton-Dickinson, Rutherford, NJ) were used as electrodes and were inserted into the dorsal midline at the anterior border of the orbit (source 1), anterior edge of the pinna (detector 1), sacral prominence at the pelvic-caudal junction (detector 2), and 4 cm from the base of the tail (source 2). Measurements of body length, tail length, source to source, and detector to detector were performed with a standard tape measure (32). Whole body resistance and whole body reactance measurements were assessed using a tetrapolar, phase-sensitive impedance analyzer (TBIA) with an 800-μA current at 50 kHz (Model 101; RJL Systems, Detroit, MI). FFM was determined using the following regression equation: FFM = [(126.66) $\times$ (source electrode distance)^2/whole body resistance] – 28.84. The TBIA procedure has a reported correlation coefficient of 0.972 compared with direct chemical analysis (32).

Glucose Tolerance, Leptin Radioimmunoassay, and Hematocrit

After 11 weeks of feeding, rats were fasted for 24 hours and were given an intraperitoneal injection of glucose (2 g/kg BW). Small blood samples were collected by tail bleeding immediately before the glucose challenge and 15, 60, and 120 minutes thereafter (33). Plasma glucose levels were determined using an Accu-Chek Easy glucometer (Boehringer Mannheim). Plasma leptin concentrations were determined using a radioimmunoassay kit (Linco Research, St. Charles, MO) (34). Plasma samples were collected from whole blood at animal death, followed by centrifugation at 1800*g* for 10 minutes at 5 °C. Hematocrit was determined with a cell counter (Cell-Dyn, Model 3500CS; Abbott Diagnostics, Santa Clara, CA).

Trace Metal Analysis

At the time of death, the right kidney and the median lobe of the liver were removed and rapidly frozen in liquid nitrogen for determination of copper content. Tissues were trimmed of fat, weighed, lyophilized, and reweighed. Copper, iron, and zinc contents of the tissue were determined by flame atomic absorption spectroscopy. Analyses of copper, iron, and zinc were verified with a certified liver standard (35).

Isolation of Cardiomyocytes

At the conclusion of the 12-week feeding period, rats were decapitated, followed by immediate removal of the hearts to isolate cardiomyocytes. Briefly, hearts were rap-

idly removed and perfused (at 37 °C) with Krebs-Henseleit bicarbonate (KHB) buffer (in mM: 118 NaCl, 4.7 KCl, 1.2 $MgSO_4$, 1.2 KH_2PO_4, 25 $NaHCO_3$, 10 HEPES, 11.1 glucose, pH 7.4). The heart was perfused for 20 minutes with KHB containing 223 U/mL collagenase II (Worthington Biochemical, Freehold, NJ) and 0.5 mg/mL hyaluronidase. After perfusion, the left ventricle was removed and minced. The cells were further digested with 0.02 mg/mL trypsin before being filtered through a nylon mesh (300 μm). Extracellular Ca^{2+} was added incrementally back to 1.25 mM. Isolated myocytes were maintained in serum-free medium for up to 12 hours after the isolation, during which time experimentation was performed (14). The myocyte yield was ~70%, with little difference among the four rat groups.

Cell Shortening/Relengthening

Mechanical properties of cardiomyocytes were assessed using an IonOptix MyoCam system (IonOptix, Milton, MA) (14). In brief, cells were superfused with a buffer containing (in mM) 131 NaCl, 4 KCl, 1 $CaCl_2$, 1 $MgCl_2$, 10 glucose, and 10 HEPES, at pH 7.4. The cells were field stimulated at 0.5 Hz. The myocyte was displayed on a computer monitor using an IonOptix MyoCam camera, which rapidly scans the image area every 8.3 ms such that the amplitude and velocity of shortening/relengthening is recorded with good fidelity. Cell shortening and relengthening were assessed using the following indices: peak shortening (PS), the amplitude myocytes shortened on electrical stimulation—indicative of peak ventricular contractility; time-to-PS (TPS), the duration of myocyte shortening—indicative of systolic duration; time-to-90% relengthening (TR_{90}), the duration to reach 90% relengthening—indicative of diastolic duration (90% rather than 100% relengthening was used to avoid noisy signal at baseline level); and maximal velocities of shortening/relengthening, maximal slope ($\pm$dL/dt; derivative) of shortening and relengthening phases—indicative of maximal velocities of ventricular pressure increase/decrease. In the case of altering stimulus frequency, a steady-state contraction of the myocyte was achieved (usually after the first five to six beats) before recording of PS. The inotropic response of myocytes to increasing concentrations of extracellular calcium (0.5 to 3.0 mM) was measured after switching the myocytes into a given extracellular Ca^{2+} concentration and pacing for 5 minutes.

Measurement of $[Ca^{2+}]_i$ Transient and Sarcoplasmic Reticulum (SR) Ca^{2+} Load

Myocytes were loaded with Fura-2/AM (0.5 μM) for 10 minutes at 30 °C, and $[Ca^{2+}]_i$ transients were recorded with a dual-excitation fluorescence photomultiplier system (Ionoptix) as described (14). Myocytes imaged through an Olympus IX-70 Fluor $\times$40 oil objective were exposed to light emitted by a 75-W lamp and passed through either a 360- or 380-nm filter (bandwidths were $\pm$15 nm) while being stimulated to contract at 0.5 Hz. Fluorescence emissions were detected between 480 and 520 nm by a photomultiplier tube after illuminating the cells first at 360 nm for 0.5 seconds and then at 380 nm for the duration of the recording protocol (333-Hz sampling rate). The 360-nm excitation scan was repeated at the end of the protocol, and qualitative changes in $[Ca^{2+}]_i$ concentration were inferred from the ratio of the fluorescence intensity at the two wavelengths. The SR Ca^{2+} loading capacity was assessed using a rapid puff of caffeine (10 mM) to induce $[Ca^{2+}]_i$ transient intensity in Fura-2–loaded ventricular myocytes. Caffeine triggers the release of Ca^{2+} from SR, the major pool of Ca^{2+} available to contractile proteins in rodent cardiac muscle. Multiple applications of caffeine were given at 5-minute intervals to ensure steady state (36).

Western Blot Analysis of Sarco(endo)plasmic Reticulum Ca^{2+}-ATPase, Phospholamban, Endothelial NO Synthase, and Signal Transducers and Activators of Transcription

Levels of sarco(endo)plasmic reticulum Ca^{2+}-ATPase (SERCA2a), phospholamban (PLB), endothelial NO synthase (eNOS), and signal transducers and activators of transcription (STAT)-3 were assessed by Western blotting. Dissected ventricular tissue was sonicated in lysis buffer containing (in mM) 10 Tris, 150 NaCl, 5 EDTA, 1% Triton X-100, and protease inhibitor cocktail followed by centrifugation at 15,000*g* for 20 minutes at 4 °C. The supernatant was transferred to a clean microtube, and protein was quantified spectrophotometrically (Molecular Diagnostics, Sunnyvale, CA) using the Bradford assay (37). Protein samples (10 μg/lane for PLB; all others, 50 μg/lane) were separated by polyacrylamide gel electrophoresis using 7% (eNOS, STAT-3) or 12% (SERCA2a, PLB) sodium dodecyl sulfate-polyacrylamide gels. Samples were transferred to polyvinylidene difluoride membranes (Pierce Biotechnology, Rockford, IL) and stained with Ponceau S red to assess equal protein loading and transfer. Membranes were blocked overnight followed by incubation (22 °C) with anti-SERCA2a (1:1000), anti-PLB (1:1000), anti-eNOS (1:1000; Transduction Laboratories, Lexington, KY), and anti-STAT-3 (1:1000; Santa Cruz Biotechnology, Santa Cruz, CA) antibodies. [Monoclonal antibodies to SERCA2a (A7R5) and PLB (2D12) were kindly provided by Dr. Larry Jones from Indiana University School of Medicine, Indianapolis, IN.] Immunoreactive bands were visualized by imaging densitometry (GS-800; Imaging Densitometer; Bio-Rad Laboratories) (14).

Ceramide Assay

Ceramide was quantified using a diacylglycerol kinase assay (38). Heart tissue was powdered under liquid nitrogen, and lipids were extracted, dried, and resolubilized in chloroform (39). An aliquot was solubilized in 20 μL of a mixed micelle solution. The reaction mixture containing 50 μL of reaction buffer (100 mM imidazole-HCl, 100 mM

LiCl, 25 mM $MgCl_2$, and 2 mM EGTA), 0.2 μL of 1 M dithiothreitol, 5 μL of diacylglycerol kinase (1 μg/μL), and 14.8 μL of dilution buffer (10 mM imidazole and 1 mM diethylenetriaminepenta-acetic acid) was added to each sample. The reaction was initiated with 10 mM [γ ^{32}P] ATP and incubated for 30 minutes at 30 °C. The reaction was terminated, and phases were separated using chloroform and perchloric acid. The lipid layer was dried under nitrogen, solubilized in chloroform, and spotted on a thin layer chromatography (TLC) plate (Whatman, Clifton, NJ). The plate was developed in a solution of chloroform:acetone: methanol:acetic acid:water (10:4:3:2:1 vol/vol) for 80 minutes. Ceramide 1-phosphate bands were identified by spraying the TLC plate with 6-(*p*-toluidino)-2-napthalenesulfonic acid (62.6 mg/200 mL in 50 mM Tris buffer, pH 7.4; Fluka, Deisenhofen, Germany) to visualize the lipid bands under low wave fluorescence light before scraping in preparation for liquid scintillation counting using a Beckman liquid scintillation counter (Beckman Instruments, Fullerton, CA).

Triglyceride Analysis

To quantify heart triglycerides (TGs), neutral lipids from an aliquot of heart lipid extract were separated by TLC developed in a solution of petroleum ether:diethylether: acetic acid (75:25:1.3 vol/vol) (14). The triglyceride bands were visualized by spraying the TLC plate with 6-(*p*-toluidino)-2-napthalenesulfonic acid, and bands corresponding to the commercial standards (NuChek Prep, Elysian, MN) were removed by scraping. After the addition of 17:0-methyl ester internal standard, TG fatty acids were subjected to transesterification by adding 0.5 M potassium hydroxide in anhydrous methanol to the silica scrapings in a test tube (40). The sample was placed in a shaking water bath for 30 minutes at 37 °C. The reaction was stopped using methyl formate, and fatty acid methyl esters were extracted using petroleum ether. After centrifugation, the top phase was removed, and the procedure was repeated. The sample was transferred to a microvial for quantification of fatty acids by gas chromatography (GC) (40). This method yields >95% conversion of TG fatty acids to methyl esters and has been used to quantify cellular TG mass (41). This conversion and recovery process was confirmed using TG standards. Total TG mass was determined by dividing the quantity of fatty acids by three and was normalized to tissue sample wet weight.

Terminal Deoxynucleotidyl Transferase–Mediated dUTP Nick-end Labeling

The terminal deoxynucleotidyl transferase–mediated dUTP nick-end labeling (TUNEL) assay was performed using a small amount (~2 mm^3) of ventricular tissue from the apex of the heart. The tissue was extracted and fixed in 4.0% buffered paraformaldehyde solution (18 °C to 24 °C, pH 7.40) and embedded in paraplast. Tissue slices of 5 μm were mounted on slides coated with poly-L-lysine (Histology Control Systems, Glen Head, NY). After deparaffinizing and dehydrating the sections, the ApopTag peroxidase in situ apoptosis detection kit (Serologicals Corp., Norcross, GA) was used to identify TUNEL-reactive cells per manufacturer's instructions. A slide of mouse mammary tissue was used as a positive control, and a negative control for each animal was created by omitting the terminal deoxynucleotidyl transferase enzyme from the assay procedure (42). Cells from tissue slices were viewed and counted in four high powered fields (×40) per slide for each rat. TUNEL-reactive cells are presented as a percentage of total cardiomyocytes viewed.

Caspase-3 Activity Assay

Caspase-3 is an enzyme activated during induction of apoptosis. Isolated cardiomyocytes were plated on 100-mm petri dishes. Caspase-3 activity was determined using the colorimetric kit purchased from R & D System (Minneapolis, MN). Myocytes were harvested and washed once with phosphate-buffered saline. After the cells were lysed, reaction buffer was added to the myocytes followed by the additional 5 μL of Caspase-3 colorimetric substrate (DEVD-pNA) and incubated in a 96-well plate for 4 hours at 37 °C in a CO_2 incubator. The plate was read with a microplate reader at 405 nm (43).

Evaluation of Protein Nitration and Lipid Peroxidation

Heart samples were homogenized in a solution containing (in mM) HEPES 20, mannitol 225, sucrose 75, and EGTA 1 at 200 rpm using a teflon pestle. The homogenate was differentially centrifuged at 3000*g* and 12,000*g* for 10 minutes each (TL-100 Ultracentrifuge; Beckman Instruments) to separate samples into mitochondrial and non-mitochondrial fractions. Mitochondrial fractions were subsequently washed with homogenization buffer and separated by centrifugation an additional two times. Mitochondrial (15 μg/lane) and non-mitrochondrial (15 μg/lane) fractions were subjected to sodium dodecyl sulfate-polyacrylamide gel electrophoresis on precast 4% to 12% polyacrylamide Tris-Glycine gels (Invitrogene Life Technologies, Carlsbad, CA). After electrophoresis, proteins were transferred to a polyvinylidene difluoride membrane (Immobilon-P; Millipore Corp., Bedford, MA) and incubated for 1 hour in the presence of rabbit anti-nitrotyrosine antibody (1:2000; Upstate, Lake Placid, NY). The blots were incubated for 1 hour in the presence of horseradish peroxidase-coupled anti-rabbit IgG (1:8000; Pierce, Rockford, IL). Proteins containing nitrotyrosine were visualized by chemiluminescence and exposure of the blots to luminescence detection film (ECL Western Blotting detection reagents and Hyperfilm-ECL; Amersham Biosciences, Piscataway, NJ). Immunoreactive bands were visualized by imaging densitometry (GS-700, Imaging Densitometer; Bio-Rad Laboratories).

Lipid peroxidation was assessed by measuring cardiac malondialdehyde levels by high-performance liquid chro-

matography. In brief, 0.5 mL of tissue suspension or a standard solution of 1,1,3,3-tetramethoxypropane was dissolved in 50 μL of ethanol containing 0.2% (wt/vol) butylated hydroxytoluene. The mixture was divided into two tubes (for duplicate determinations), and to each tube, 1.5 mL of 0.44 M H_3PO_4 was added. After 10 minutes at room temperature, 0.5 mL of 0.6% (wt/vol) thiobarbituric acid solution was added to the samples, which were heated gently to 60 °C to dissolve the thiobarbituric acid. The samples were heated to 90 °C for 45 minutes and cooled on ice. The mixture was centrifuged at 4 °C at 6000 rpm for 5 minutes, and the supernatant was removed and filtered with a 0.2-μm Gelman polytetrafluroethylene syringe filter (Pall Life Sciences, Ann Arbor, MI) to remove particulate matter. The filtered supernatant (20 μL) was injected onto a Waters Symmetry column (C18, 5.0 μm particle size, 4.6 mm $\times$ 250 mm; Waters, Milford, MA) using a Shimadzu Model SCL 10-A VP high-performance liquid chromatography system fitted with a Shimadzu SIL-10A autoinjector (Shimadzu, Columbia, MD) and eluted with a mobile phase made up of 65% 50 mM KH_2PO_4 (adjusted to pH 7.0 with 3 M KOH) and 35% methanol. The flow rate was 1 mL/min. The malondialdehyde peak eluted at 8 minutes and was detected using a Waters 474 scanning fluorescence detector with excitation at 532 nm and emission at 553 nm (44).

Aconitase Activity Assay

Aconitase is an iron-sulfur enzyme located in the cytosol and mitochondrial citric acid cycle. The catalytically active form of aconitase contains a [4Fe-4S] cluster interacting with carboxyl and hydroxyl groups of substrates. Mitochondrial and cytosolic aconitase are readily damaged by oxidative stress through the removal of an iron from the [4Fe-4S] clusters. The Fe atom may be removed by any of the oxidants including superoxide, hydrogen peroxide, NO, or peroxynitrite (45). Thus, aconitase activity is used as a sensitive marker for oxidative damage. Mitochondrial fractions were prepared from whole heart tissue homogenate as previously described for the nitrotyrosine assay (14). After protein concentration was determined using the bicinchoninic acid protein assay kit (Pierce Biotechnology), the Aconitase-340 assay (OxisResearch, Portland, OR) was performed per manufacturer instructions. Briefly, the mitochondrial sample (200 μL) was mixed in a cuvette with 200 μL trisodium citrate in Tris-HCl, pH 7.4, 200 μL isocitrate dehydrogenase in Tris-HCl, and 200 μL $NADP^+$ in Tris-HCl. After incubating for 15 minutes at 37 °C, absorbance was recorded at 340 nm for 5 minutes on a spectrophotometer. During the assay, citrate was isomerized by aconitase into isocitrate and eventually converted to α-ketoglutarate. The Aconitase-340 assay (OxisResearch) measures reduced nicotinamide adenine dinucleotide phosphate, a byproduct of the conversion of isocitrate to α-ketoglutarate. Tris-HCl buffer (pH 7.4) was used as a blank.

Electron Transport Chain Enzymatic Activity [CCO, Reduced Nicotinamide Adenine Dinucleotide (NADH)/ Succinate Cytochrome c Reductase]

Ventricular homogenate was centrifuged at 600*g* for 10 minutes. After the pellet was discarded, the supernatant was centrifuged at 7700*g* for 10 minutes. The resulting mitochondrial pellet was washed once and resuspended. NADH: cytochrome c reductase, succinate:cytochrome c reductase, and CCO activities were assayed at 30 °C in isolated mitochondria by a sequential, continuous assay that allows measurement of all three enzyme activities in a single sample of mitochondria (46). Briefly, CCO activity was measured by monitoring the change in absorbance at 550 nm (ΔA_{550}) resulting from the oxidation of reduced cytochrome c. The CCO activity was monitored until ΔA_{550} was ~0.6 U, at which point CCO activity was terminated by adding potassium cyanide (0.17 mM). Succinate (12.5 mM) was added, and succinate:cytochrome c reductase activity was measured by monitoring ΔA_{550}, resulting from the reduction of the cytochrome c previously oxidized by CCO. Succinate: cytochrome c reductase activity was terminated by adding malonate (17 mM), and NADH:cytochrome c reductase activity was measured by adding NADH (2.8 nM) and monitoring ΔA_{550}, resulting from the further reduction of cytochrome c. The rate of cytochrome c oxidation or reduction (nmoles per minute) was calculated using a molar extinction coefficient of 19,600 for cytochrome c (47).

Statistical Analysis

Data are mean $\pm$ standard error (SE). Statistical significance ($p < 0.05$) for each variable was estimated by two-way ANOVA followed by Tukey's post hoc test where appropriate.

Results

General Features of Experimental Animals

A high-fat diet significantly increased body weight gain, whereas marginal copper deficiency did not affect body weight gain. A significant separation of body weight was observed between the high-fat and low-fat diet groups, regardless of copper status, after 6 weeks and continued throughout the duration of the study (Figure 1A). Notably, daily food consumption records revealed a significantly higher dietary intake (average grams per day) of animals consuming low-fat diets, regardless of copper concentration (LFCuA: 18.8 $\pm$ 0.5 g/d; LFCuD: 19.9 $\pm$ 0.4 g/d; HFCuA: 15.7 $\pm$ 0.4 g/d; HFCuD: 16.3 $\pm$ 0.4 g/d; $p < 0.05$ between low- and high-fat groups). Figure 1B exhibits a weekly diet intake chart among the four experimental groups. However, because high-fat diets were calorically enriched, the overall caloric consumption was similar for all but 2 weeks during the feeding period, thus resulting in no difference in overall caloric consumption among the four rat groups (LFCuA: 73.6 $\pm$ 2.0 kcal/wk; LFCuD: 77.8 $\pm$ 2.1 kcal/wk; HFCuA:

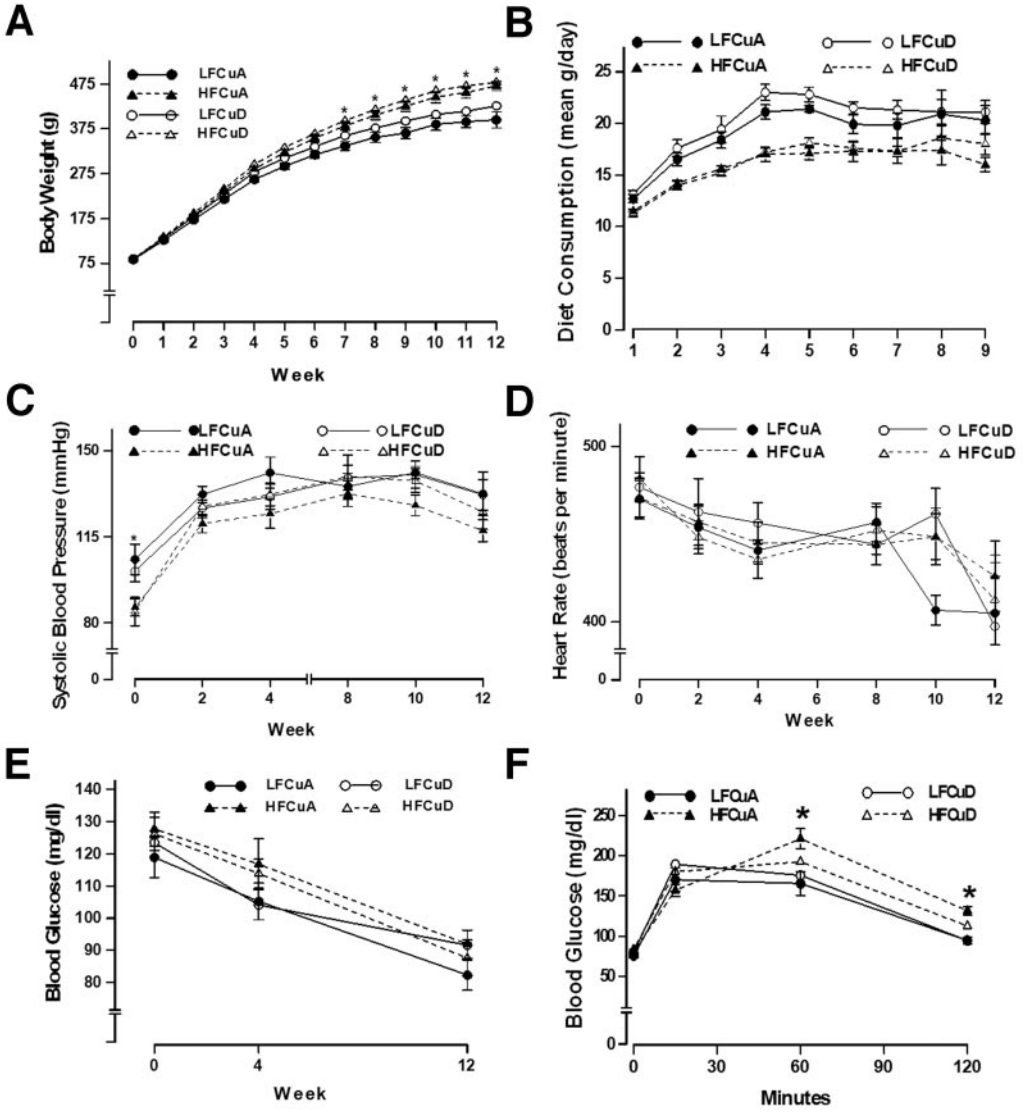

Figure 1: (A) Weekly body weight, (B) daily diet consumption, (C) systolic blood pressure, (D) heart rate, (E) blood glucose, and (F) intraperitoneal glucose tolerance test (2 g/kg body weight) at the end of week 11 in rats fed LFCuA, LFCuD, HFCuA, and HFCuD diets for 12 weeks. Mean ± SE, $n = 9$ to 10 rats per group. * $p < 0.05$ vs. low-fat/copper-adequate diet group.

76.1 ± 1.8 kcal/wk; HFCuD: 78.6 ± 2.0 kcal/wk; $n = 3$ to 5 rats/group; $p > 0.05$). Neither a high-fat nor a marginally copper-deficient diet significantly affected systolic BP (Figure 1C), heart rate (Figure 1D), or fasting blood glucose (Figure 1E) throughout the duration of the study. Interestingly, a glucose tolerance test conducted 1 week before death (after 11 weeks of feeding) indicated compromised glucose tolerance in the high-fat/copper-adequate diet group, consistent with the notion that obesity is often accompanied by insulin resistance (48). After an intraperitoneal glucose challenge (2 g/kg body weight), plasma glucose levels of low fat-fed rats increased and rapidly returned close to the baseline value within 120 minutes. However, the postchallenge glucose levels remained elevated in the high-fat/copper-adequate rats at 60 and 120 minutes compared with the rats fed a low-fat diet (Figure 1F), indicating whole body insulin resistance. Marginal copper deficiency did not affect glucose tolerance in the low-fat diet group but somehow neutralized high fat diet-induced glucose tolerance. High fat diet-fed animals were euglycemic and hyperleptinemic, regardless of copper status, but did not display any overt organomegaly, with the exception of increased absolute heart weight (which parallels with increase body weight) in the high-fat diet groups. Hematologic analysis revealed comparable levels of hematocrit, hemoglobin, and red blood cell distribution width in all four dietary groups, excluding hematologic abnormality after these dietary maneuvers (Table 2).

Table 2. Biometric and hematologic data of animals after 12 weeks of consuming a high-fat diet, a marginally copper-deficient diet, or both

	LFCuA	LFCuD	HFCuA	HFCuD
BW (g)	395.0 ± 17.9	426.4 ± 14.6	471.0 ± 10.2*	479.2 ± 14.8*
Heart weight (g)	1.39 ± 0.06	1.44 ± 0.08	1.56 ± 0.07*	1.57 ± 0.07*
Heart weight/BW (mg/g)	3.69 ± 0.25	3.39 ± 0.20	3.49 ± 0.17	3.29 ± 0.15
Liver weight (g)	12.23 ± 0.81	13.58 ± 0.81	13.96 ± 0.79	14.90 ± 1.13
Kidney weight (g)	2.69 ± 0.11	2.72 ± 0.12	2.85 ± 0.10	2.92 ± 0.09
Hematocrit (%)	41.94 ± 1.28	43.28 ± 0.78	43.62 ± 1.08	43.96 ± 0.21
Hemoglobin (g/dl)	14.16 ± 0.54	15.48 ± 0.39	15.42 ± 0.39	15.28 ± 0.24
RBC distribution width	15.68 ± 0.32	16.72 ± 0.53	15.60 ± 0.06	14.74 ± 0.32
Plasma glucose (mM)	4.57 ± 0.26	5.09 ± 0.46	5.11 ± 0.24	4.86 ± 0.31
Plasma leptin (ng/mL)	4.42 ± 0.58	3.71 ± 0.39	7.97 ± 0.98*	7.84 ± 0.67*

LFCuA, low-fat, copper-adequate diet; LFCuD, low-fat, marginally Cu^{2+}-deficient diet; HFCuA, high-fat, copper-adequate diet; HFCuD, high-fat, marginally Cu^{2+}-deficient diet; RBC, red blood cell. Mean ± standard error.
* $p < 0.05$ vs. corresponding low-fat group, $n = 10$ rats per group.

After the 12-week feeding regimen, consumption of the marginally copper-deficient diet significantly reduced kidney copper concentrations, regardless of dietary fat status. The liver copper levels were also significantly decreased, although this decline seems to be related to dietary fat. Interestingly, the high-fat diet significantly enhanced renal and hepatic iron levels. Zinc levels were not affected by either diet treatment (Table 3). It should be cautioned that the trace metal concentration may be diluted and biased by elevated lipid storage after high-fat diet intake (20). Nonetheless, the fact that liver and kidney weights were not significantly altered after high-fat intake (Table 2) does not support lipid accumulation in those organs after high-fat diet intake.

From estimation of body composition using TBIA, we found that the obesity index [cubic root of body weight in g divided by body length in meters, equivalent to BMI in humans (49)], body length, total body water, FFM and FM, and fat percentage were not significantly different among the four rat groups after 12 weeks of high-fat and/or marginally copper-deficient dietary feeding (Table 4).

Effect of HFCuD Diets on Tissue Oxygen Consumption, Tissue Levels of TGs, Ceramide, Lipid Peroxidation, and Apoptosis

Lipotoxicity plays an essential role in compromised cardiac function in genetically obese *fa/fa* rats (6). Hallmarks of lipo-

Table 3. Renal and hepatic concentrations of copper, iron, and zinc after 12 weeks of diet feeding containing various levels of copper and fat

	LFCuA	LFCuD	HFCuA	HFCuD
Kidney $copper^{2+}$ (μg/g)	43.7 ± 4.6	31.2 ± 2.5†	43.1 ± 2.4	32.4 ± 2.6†
Kidney iron (μg/g)	248.4 ± 4.4	261.9 ± 14.8	279.3 ± 7.9*	278.4 ± 6.3*
Kidney zinc (μg/g)	104.4 ± 2.1	99.2 ± 4.2	104.5 ± 1.9	105.7 ± 1.6
Liver $copper^{2+}$ (μg/g)	13.4 ± 0.6	13.2 ± 0.7	12.7 ± 0.3*	10.7 ± 0.5*
Liver iron (μg/g)	287.8 ± 15.4	407.4 ± 40.5	399.7 ± 18.3*	374.4 ± 25.5*
Liver zinc (μg/g)	88.6 ± 9.0	94.0 ± 2.0	87.3 ± 2.6	77.4 ± 4.4
Dietary $copper^{2+}$ (ppm)	5.04 ± 0.36	1.40 ± 0.14†	6.56 ± 0.46	1.68 ± 0.33†

LFCuA, low-fat, copper-adequate diet; LFCuD, low-fat, marginally Cu^{2+}-deficient diet; HFCuA, high-fat, copper-adequate diet; HFCuD, high-fat, marginally Cu^{2+}-deficient diet. Mean ± standard error.
* $p < 0.05$ vs. corresponding low-fat group.
† $p < 0.05$ vs. copper-adequate groups, $n = 9$ to 10 rats per group.

Table 4. Bioimpedance data of rats after 12 weeks of diet feeding containing various levels of copper and fat

	LFCuA	LFCuD	HFCuA	HFCuD
FFM (g)	309.2 ± 20.8	364.3 ± 16.5	366.8 ± 15.1	382.0 ± 11.5
FM (g)	75.8 ± 14.6	51.5 ± 6.4	90.4 ± 11.5	82.2 ± 12.3
Fat percentage (%)	20.0 ± 3.7	12.9 ± 1.7	19.7 ± 2.4	17.5 ± 2.3
Total body water (g)	228.8 ± 14.3	266.8 ± 11.4	268.5 ± 10.4	279.0 ± 7.9
Body length (cm)	24.4 ± 0.2	25.2 ± 0.2	25.3 ± 0.3	26.0 ± 0.3
Obesity index	299.8 ± 2.2	295.9 ± 2.8	304.0 ± 2.8	298.9 ± 2.3

LFCuA, low-fat, copper-adequate diet; LFCuD, low-fat, marginally Cu^{2+}-deficient diet; HFCuA, high-fat, copper-adequate diet; HFCuD, high-fat, marginally Cu^{2+}-deficient diet; FFM, fat-free mass; FM, fat mass. Mean ± standard error, $n = 9$ to 10 rats per group. Obesity index was calculated as the cubic root of body weight in grams divided by body length in meters.

toxicity entail altered oxygen metabolism, elevated levels of TGs and ceramide, lipid peroxidation, and apoptosis. Data presented in Figure 2 reveal similar levels of oxygen consumption and tissue levels of TGs and ceramide among all four diet groups. Although no significant difference was detected for TG levels among the four experimental groups, a significant difference was observed when comparing fat or copper content individually (low-fat groups: 0.47 ± 0.04 nM/mg tissue vs. high-fat groups: 0.62 ± 0.04 nM/mg tissue; $n = 9$ to 10 hearts; $p < 0.05$ between the two fat groups; copper-adequate groups: 0.63 ± 0.04 nM/mg tissue vs. marginally copper-deficient group: 0.45 ± 0.04 nM/mg tissue; $n = 9$ to 10 hearts; $p < 0.05$ between the two copper groups). Evaluation of apoptosis using either caspase-3 activity or TUNEL assay did not reveal any significant alteration in cell survival in all four diet groups studied (Figure 2E and F). Collectively, these data suggest that rat hearts after 12 weeks of the high-fat and/or marginally copper-deficient diet feeding regimen are unlikely to possess characteristics of lipotoxicity.

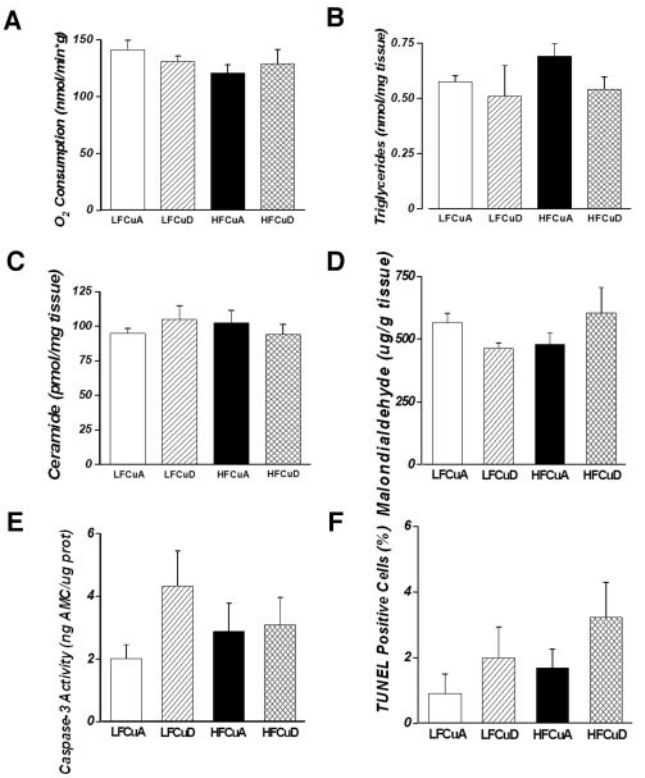

Figure 2: (A) Oxygen consumption, (B) triglycerides, (C) ceramide, (D) malondialdehyde, (E) caspase-3 activity, and (F) TUNEL apoptosis in heart tissues from animals fed with LFCuA, LFCuD, HFCuA, and HFCuD diets for 12 weeks. Mean ± SE, $n =$ 4 to 5 rats per group.

Effect of High Fat and Marginal Copper Deficiency on Cardiomyocyte Function and $[Ca^{2+}]_i$

The average cell length used in this study was 116.4 ± 1.3 μm ($n = 208$ cells) for the LFCuA group, 112.7 ± 1.3 μm ($n = 207$ cells) for the LFCuD group, 117.5 ± 1.3 μm ($n = 208$ cells) for the HFCuA group, and 121.2 ± 1.3 μm ($n = 208$ cells) for the HFCuD group. A representative trace depicting the effect of 12 weeks of high-fat and/or marginally copper-deficient diet feeding on myocyte shortening is shown in Figure 3A. Rats fed with either a high-fat or marginally copper-deficient diet exhibited depressed PS and ±dL/dt, as well as prolonged TR_{90}. There was no additive or synergistic effect between the two diets on PS, ± dL/dt, and TR_{90}. TPS was not significantly affected by the two dietary treatments either alone or in combination (Figure 3). The $[Ca^{2+}]_i$ fluorescence indicator Fura-2 was used to evaluate $[Ca^{2+}]_i$ handling properties in cardiomyocytes obtained from rats fed with high-fat and/or marginally copper-deficient diets. The resting $[Ca^{2+}]_i$ and SR Ca^{2+} load measured by caffeine-induced Ca^{2+} release were not different in cardiomyocytes from the four dietary groups. However, both diet treatments significantly reduced electrically

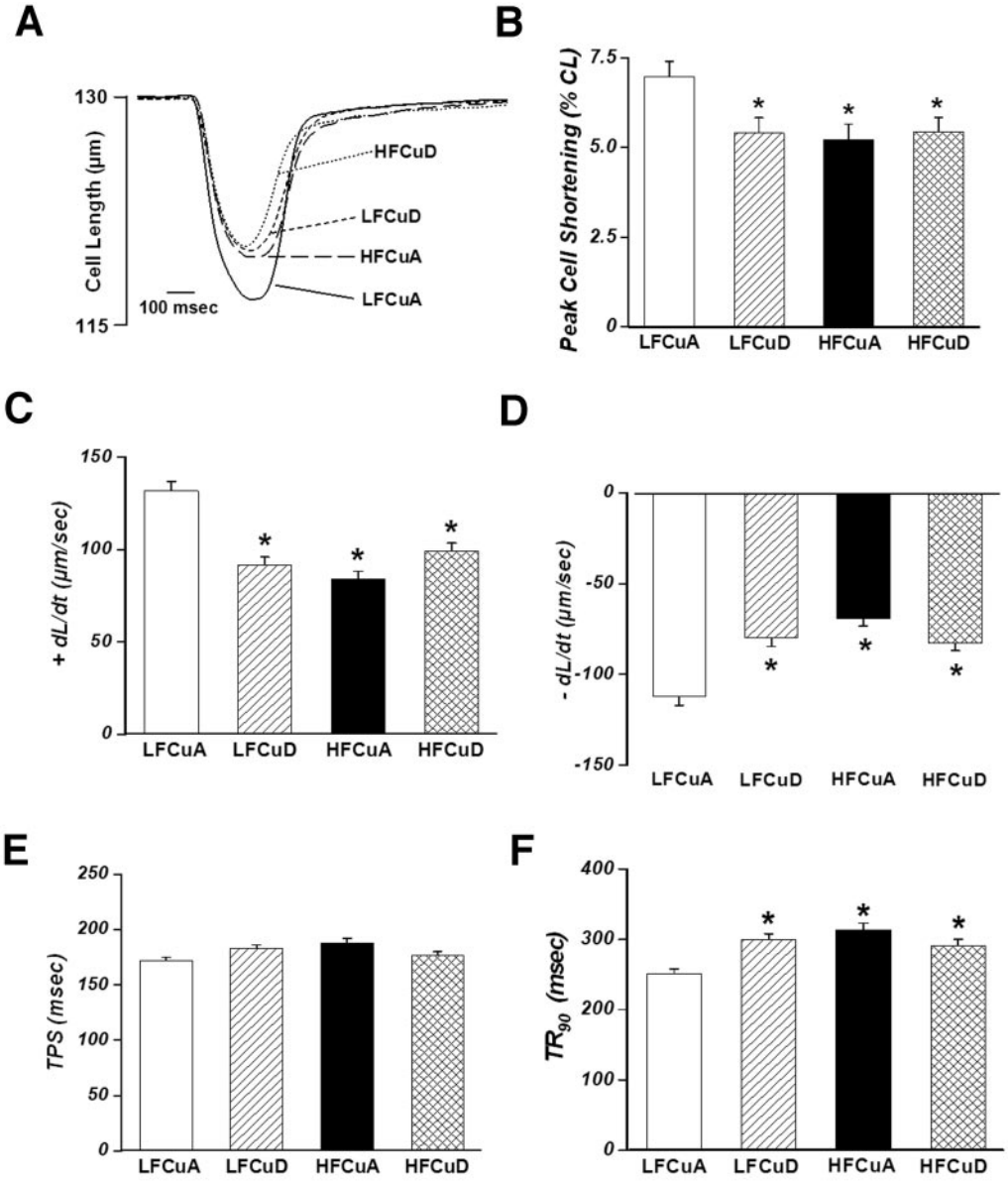

Figure 3: Effect of HFCuD diets on cell shortening in cardiomyocytes. (A) Representative traces depicting cell shortening from LFCuA, LFCuD, HFCuA, and HFCuD groups. (B) PS (percent of resting cell length). (C) +dL/dt. (D) −dL/dt. (E) TPS. (F) TR_{90}. Mean ± SE, n = 207 to 208 myocytes from five animals per group. * $p < 0.05$ vs. LFCuA group.

induced increases in $[Ca^{2+}]_i$ levels ($\Delta[Ca^{2+}]_i$) and prolonged $[Ca^{2+}]_i$ decay rate without additive effects between the two dietary treatments (Figure 4).

Effect of High Fat and Marginal Copper Deficiency on Cardiomyocyte Ca^{2+} and Frequency Response

To further delineate the mechanism responsible for depressed PS and ±dL/dt after high-fat and/or marginally copper-deficient diets, peak cell shortening was re-examined in cardiomyocytes exposed to increasing stimulus frequencies (0.1 to 5.0 Hz) or extracellular Ca^{2+} concentrations (0.5 to 3.0 mM). Increasing stimulus frequency from 0.1 to 5.0 Hz gradually depressed PS to greater extents in myocytes from high fat, marginal copper deficiency, or both dietary groups in combination. There was no additive effect between both diet treatments (Figure 5A). These data indicate that high-fat and marginally copper-deficient diets may compromise SR Ca^{2+} re-uptake or re-sequestration in cardiomyocytes under high stress. On the other hand, changing extracellular Ca^{2+} concentration from 0.5 to 3.0 mM augmented PS amplitude in a

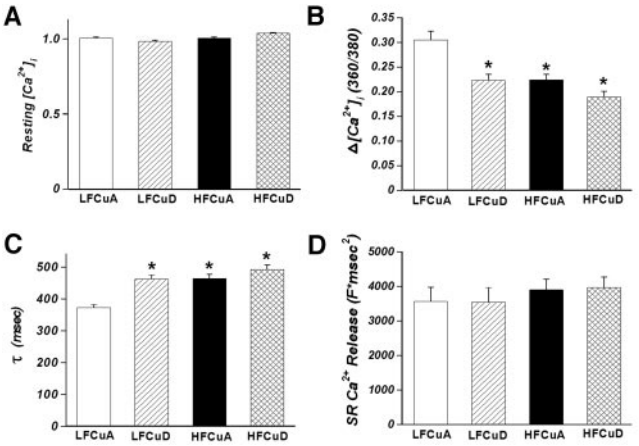

Figure 4: Effect of HFCuD diets on $[Ca^{2+}]_i$ properties in cardiomyocytes. (A) Baseline $[Ca^{2+}]_i$ levels, (B) electrically stimulated increase in $[Ca^{2+}]_i$ ($\Delta[Ca^{2+}]_i$), (C) $[Ca^{2+}]_i$ transient decay rate (τ), and (D) caffeine (10 mM)-triggered SR Ca^{2+} release in myocytes from LFCuA, LFCuD, HFCuA, and HFCuD groups. Mean ± SE, $n = 117$ to 118 (20 to 27 for D) cells from five rats. * $p < 0.05$ vs. LFCuA group.

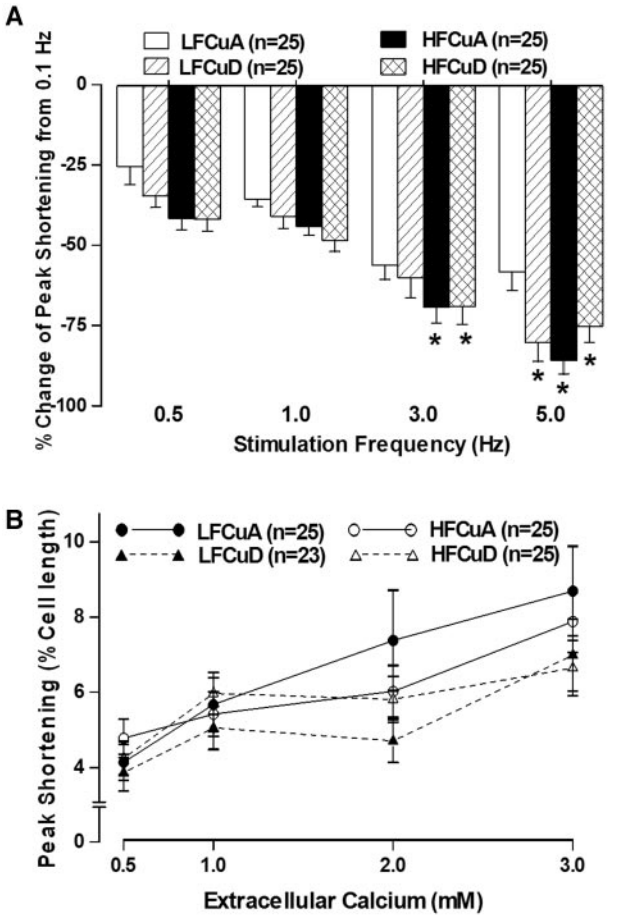

Figure 5: Effect of increasing (A) stimulating frequency (0.1 to 5.0 Hz) and (B) extracellular Ca^{2+} concentration (0.5 to 3.0 mM) on myocyte shortening amplitude (PS) in cardiomyocytes from LFCuA, LFCuD, HFCuA, and HFCuD groups. Mean ± SE, $p < 0.05$ vs. LFCuA group; numbers in parentheses indicate number of myocytes used in the study.

comparable manner in all groups tested, suggesting similar Ca^{2+} responsiveness in cardiomyocytes in response to either dietary treatment (Figure 5B).

Effect of High-fat and Marginally Copper-deficient Diets on SERCA2a, PLB, eNOS, and STAT-3

$[Ca^{2+}]_i$-cycling proteins SERCA and PLB play a significant role in maintaining normal cardiomyocyte excitation-contraction coupling (50). Altered $[Ca^{2+}]_i$ transients (Figure 4) and dampened PS frequency response (Figure 5A) in high-fat and marginally copper-deficient diets indicated possible derangement of $[Ca^{2+}]_i$ homeostasis. To examine the influence of high-fat and marginally copper-deficient diets on $[Ca^{2+}]_i$ cycling proteins, abundance of SERCA2a and PLB was determined. Cardiac expression of SERCA2a was similar among all four dietary groups (Figure 6A). However, expression of PLB, which serves as a "lock" for SERCA2a, was significantly elevated in high-fat and marginally copper-deficient diet groups. Combination of both diets did not produce further increase of PLB protein expression (Figure 6B). The ratio of SERCA2a/PLB was significantly reduced in the marginally copper-deficient group only (data not shown). Although obesity is often associated with increased NOS activity and NO availability (10,51), en route to nitrosative damage, no difference in eNOS expression was observed among the four dietary groups (Figure 6C). In our study, a high-fat diet induced hyperleptinemia, regardless of copper status, indicating possible alteration of leptin signaling. Leptin signaling including the postreceptor signaling pathway Janus kinase/STAT has been shown to play an essential role in cardiac structure and contractile function (34,52). To explore possible contribution of leptin signaling in high-fat and marginally copper-deficient diets to cardiomyocyte contractile dysfunction under these dietary conditions, levels of STAT-3 were examined, and our results showed comparable STAT-3 expression among all four dietary groups (Figure 6D).

Effect of High-fat and Marginally Copper-deficient Diets on the Electron Transport Chain and Mitochondrial Function

CCO, the terminal respiratory complex (complex IV) of the mitochondrial respiratory chain, is a copper-dependent enzyme. Hepatic CCO activity has been shown to be reduced during copper deficiency (47). Reduction in CCO activity may contribute to oxidative stress under copper deficiency by promoting increased mitochondrial

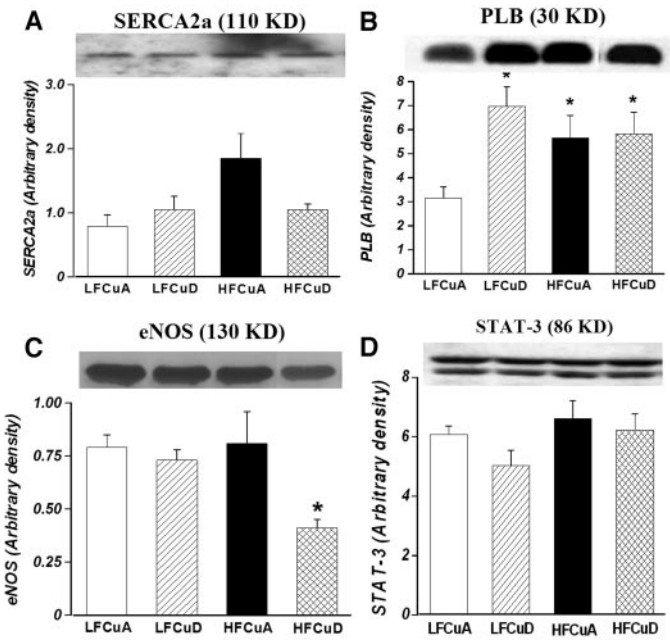

Figure 6: Effect of 12-week high-fat and/or marginally copper-deficient dietary feeding on (A) SERCA2a, (B) PLB, (C) eNOS, and (D) STAT-3 levels in hearts. (Insets) Representative immunoblots using specific anti-SERCA2a, anti-PLB, anti-eNOS, and anti-STAT-3 antibodies. Mean ± SE, $n = 3$ to 4 hearts/group. * $p < 0.05$ vs. LFCuA group.

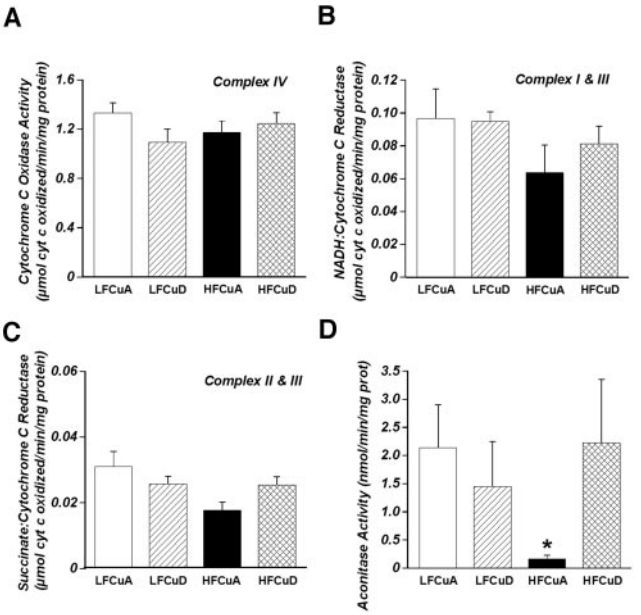

Figure 7: Effect of 12-week high-fat and/or marginally copper-deficient dietary feeding electron respiratory chain and mitochondrial damage in hearts. (A) CCO activity, (B) complex I and II, (C) complex I and III, and (D) aconitase activity. Mean ± SE, $n = 5$ hearts/group. * $p < 0.05$ vs. LFCuA group.

reactive oxygen species feneration. Nonetheless, data from our study revealed comparable cardiac CCO in high-fat and/or marginally copper-deficient diet groups (Figure 7A). To determine whether a high-fat and marginally copper-deficient diet, alone or in combination, affected mitochondrial respiratory complex activities other than CCO, NADH:cytochrome c reductase, which represents combined activities of respiratory complexes I and III, and succinate:cytochrome c reductase, which represents the combined activities of respiratory complexes II and III, were evaluated in hearts of high-fat and/or marginally copper-deficient diet groups. Consistent with their effects on CCO activity, neither dietary regimen, alone or in combination, affected NADH:cytochrome c reductase (Figure 7B) or succinate:cytochrome c reductase (Figure 7C) enzymatic activities. These findings do not support alteration in the electron transport chain under high-fat and/or marginally copper-deficient diet treatments. Interestingly, mitochondrial aconitase activity was significantly reduced in high-fat but not marginally copper-deficient or combined diet groups (Figure 7D). Mitochondrial aconitase, an iron-sulfur enzyme located in the citric acid cycle, is readily damaged by oxidative stress through removal of an iron from [4Fe-4S] cluster (45).

Effect of High-fat and Marginally Copper-deficient Diets on Protein Nitration

Increased protein nitration has been reported in obesity, resulting from increased NOS activity and NO availability (10,51). Similarly, changes in cardiac NOS activity and/or protein expression have also been indicated under dietary copper deficiency (53). To evaluate cardiac protein nitration and nitrosative stress after high-fat and/or marginally copper-deficient diet feeding, nitrotyrosine level was measured. Results shown in Figure 8 display a comparable degree of protein nitration among all four dietary groups, indicating unlikely presence of nitrosative protein damage after high-fat and/or marginally copper-deficient diet treatment.

Discussion

Copper deficiency may progress to various intensities, depending on copper levels in the diet. Adequate level of copper in rodents is usually 5 to 6 ppm. Under severe copper deficiency, in which rodent diets offer only ~0.5 ppm, activity of copper-dependent enzymes is dramatically attenuated, resulting in premature death within 6 to 8 weeks (24,53). To circumvent such limitations in a chronic study such as the 12-week feeding used in this work, marginal levels of dietary copper were introduced to achieve marginal copper deficiency (54–56). However, a consensus on the definition of "marginal copper deficiency" has not been well established. Marginal levels of dietary copper have

A

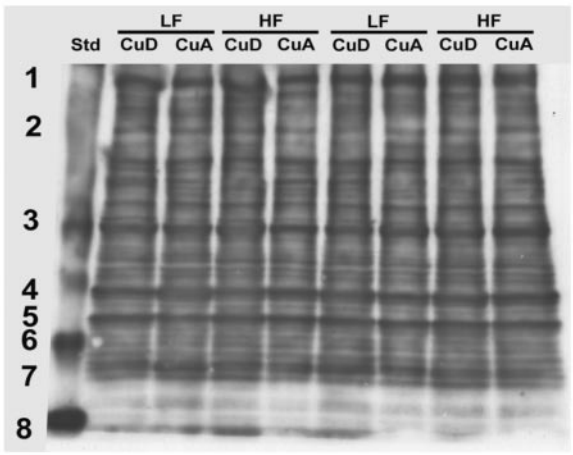

B

Band (Rf)	LFCuA (OD ratio)	LFCuD (OD ratio)	HFCuA (OD ratio)	HFCuD (OD ratio)
Band #1	0.6 ± 0.1	0.7 ± 0.1	0.6 ± 0.0	0.4 ± 0.1
Band #2	1.2 ± 0.2	1.0 ± 0.1	0.9 ± 0.0	0.9 ± 0.1
Band #3	1.3 ± 0.4	0.9 ± 0.1	0.8 ± 0.1	0.9 ± 0.1
Band #4	1.6 ± 0.6	1.1 ± 0.1	1.0 ± 0.1	1.0 ± 0.1
Band #5	1.9 ± 0.8	1.2 ± 0.1	1.2 ± 0.1	1.2 ± 0.1
Band #6	1.8 ± 1.0	0.9 ± 0.1	0.8 ± 0.0	0.8 ± 0.1
Band #7	2.1 ± 1.2	1.0 ± 0.1	1.0 ± 0.1	1.0 ± 0.0
Band #8	1.9 ± 1.5	0.6 ± 0.1	0.5 ± 0.1	0.5 ± 0.1

Figure 8: Effect of 12-week high-fat and/or marginally copper-deficient dietary feeding on nitrotyrosine protein expression in ventricular tissues. (A) Actual gel blotting. (B) Pooled data of arbitrary optical density of bands 1 through 8 shown on A. Mean ± SE, $n = 4$ to 5 animals/group. $p > 0.05$.

been defined as 50% to 60% of the recommended intake (54,56). Animals subsisting on 30% of recommended copper levels, as used in this study, do not succumb to cardiac aneurysms or severe cardiomyopathy (24,53). Levels of tissue copper, the "gold standard" of copper deficiency and copper-dependent enzymes, may vary depending on dietary copper content. In this study, 1.4 ppm of copper (28% of adequate copper content) was introduced to rats for 12 weeks, resulting in reduced renal but not hepatic copper levels. Intriguingly, liver copper content was reduced by dietary fat content, consistent with the notion that obesity itself may lead to decreased copper levels (21). Marginal copper diets using higher levels of copper (2.5 ppm) displayed similar effects on hepatic copper when dietary fat was increased (54,56). Therefore, the combination of high-fat and marginally copper-deficient diet may place organs at much greater risk of copper deficiency than either diet alone. However, data should be interpreted with caution because increased lipid accumulation in a given organ may unduly dilute the concentration of copper expressed per gram of organ weight (20).

This study provided evidence that high-fat and/or marginally copper-deficient diets induce depression of cardiomyocyte contractile capacity (PS and $\pm$dL/dt) and prolongation of diastolic duration (TR_{90}) without any additive effect between the two diets. Furthermore, diet-induced mechanical dysfunctions are associated with reduced electrically-stimulated $[Ca^{2+}]_i$ rise ($\Delta[Ca^{2+}]_i$), slowed $[Ca^{2+}]_i$ clearing rate (τ), and enhanced expression of the Ca^{2+}-cycling protein PLB. These effects elicited by high-fat and/or marginally copper-deficient diets are supported by dampened PS-stimulus frequency response, again without any additive effect between the two diets. In addition, compromised cardiomyocyte mechanical properties (PS, $\pm$dL/dt, TR_{90}, dampened PS-stimulus frequency response, $\Delta[Ca^{2+}]_I$, and τ) developed in the absence of changes in cardiomyocyte Ca^{2+}-sensitivity, SR Ca^{2+} load, and resting $[Ca^{2+}]_i$ levels. Although up-regulated PLB seems to offer an explanation for $[Ca^{2+}]_i$ mishandling and cardiomyocyte dysfunction under high-fat and/or marginally copper-deficient diets, our data did not favor any involvement of SERCA2a and postleptin receptor STAT-3 signaling in high-fat and/or marginally copper-deficient diet-induced cardiomyocyte dysfunction. No change in tissue levels of TG, ceramide, and malondialdehyde was noted, excluding the possible contribution of lipotoxicity and lipid peroxidation to high fat– and/or marginal copper deficiency–induced cardiac defects. Negative findings from caspase-3 and TUNEL assays, electron transport chain (complex I–IV), and oxygen consumption seem to rule out participation of lipoapoptosis, mitochondrial respiration, and oxygen metabolism in high fat– and/or marginal copper deficiency–induced cardiomyocyte contractile and $[Ca^{2+}]_i$ dysregulation. Lack of additive or synergistic effect between high fat and marginal copper deficiency in most of the experimental parameters indicates that the two dietary treatments may compromise cardiac contractile and $[Ca^{2+}]_i$ properties through a somewhat similar or shared mechanism, at least in this experimental setting.

Cardiomyopathy may be triggered by multiple initiating culprit factors including obesity (5,9,14,57), copper deficiency (19,24), hypertension, and diabetes (58,59). One of the classic features of cardiomyopathy is hypertrophied chambers, which eventually lead to congestive heart failure. The hypertrophied and failing heart exhibits early signs of impaired contractile function and $[Ca^{2+}]_i$ homeostasis (60). Cardiac hypertrophy, interrupted cardiac excitation-contraction coupling, and elevated PLB expression were seen in this study. Intriguingly, a more severe decline of PS stimulus frequency response, which is crucial to identify heart failure (60), was present in cardiomyocytes from high-fat and/or marginally copper-deficient groups. Up-regulated PLB, a negative regulator of SERCA2a, has been shown to contribute to depressed PS, $\pm$dL/dt, $\Delta[Ca^{2+}]_i$, prolonged TR_{90}, and τ, as well as a more severe negative PS stimulus frequency response (60,61). It should be pointed out that evaluation of PLB protein abundance in the absence of phosphorylation and kinetic data may obscure ap-

propriate interpretation (60,62). Non-phosphorylated PLB inhibits SERCA-induced Ca^{2+} reuptake, the inhibitory effect of which can be relieved by its phosphorylation at Ser16 or Thr17 sites (62). Further study is warranted to examine the activity and abundance of protein phosphatases and the phosphorylation states of PLB to better understand its role in high-fat diet and/or marginal copper deficiency-induced cardiomyocyte contractile and $[Ca^{2+}]_i$ dysfunctions. Last, but not least, it should be noted that dietary copper status affects cardiac function through regulation of neurotransmitters such as catecholamines (63), which may contribute to the interaction of copper status and obesity on cardiac function.

Lipotoxicity has been proposed to play an essential role in obesity and hyperlipidemia-induced heart dysfunctions (6,15). Increased lipid deposit (54,56), depressed contractile function (24,27), elevated NO levels (53), and apoptosis (28) have been shown to parallel lipotoxic cardiac dysfunction (6). Nevertheless, neither marginal copper deficiency nor high fat, alone or in combination, induced significant elevation in ceramide, lipotoxic markers, or a sphingolipid central to metabolism and synthesis of many other sphingolipids. Although a high-fat diet and marginal copper deficiency alone enhanced and reduced cardiac TG levels, respectively, the fact that TG levels were not significantly different among the four dietary groups does not support a lipotoxic condition in this study. This is consistent with unaltered tissue ceramide levels from our study. In fact, a marginally copper-deficient diet (regardless of the fat status) significantly reduced tissue TG levels from 0.63 ± 0.04 to 0.45 ± 0.04 nmol/mg tissue, further ruling out the possible contribution of lipotoxicity in the pathogenesis of marginal copper deficiency-induced cardiomyopathy. Our observation of unchanged eNOS protein expression in high-fat and marginal copper deficiency groups is in support of the negative finding of nitrotyrosine staining in all experimental groups, excluding a possible contribution of nitrosative damage to high-fat and/or marginally copper-deficient diet-induced cardiomyocyte defects. Interestingly, the combined dietary regimen of high fat and marginal copper deficiency suppressed eNOS expression, with little effect when either diet was used alone, indicating possible interation between the two diets on NOS transcription and translation. Measurement of electron transport chain enzymatic activities revealed no alteration in CCO (complex IV), NADH:cytochrome c reductase (complex I and III), or succinate:cytochrome c reductase (complex II and III) among the four dietary groups, which does not support the presence of oxidative stress. The lack of contribution of oxidative stress in our study is consistent with negative findings in lipid peroxidation and apoptosis. However, our data revealed depressed mitochondrial aconitase activity after high-fat feeding, somewhat contrary to what was seen in the electron transport chain. Possible differences in methodology may contribute to this apparent discrepancy in mitochondrial function. Aconitase is associated with isomerization of citrate to isocitrate within the citric acid cycle, leading to conversion of isocitrate to oxalosuccinate and production of NADH. Although NADH is a substrate for the electron transport chain, our method used to examine mitochondrial complexes in this study relied essentially on exogenous NADH rather than NADH supplied by mitochondria.

It should be mentioned that elevated TG and fatty acid levels have been reported in high-fat feeding (64), and these stimulate serine palmitoyl transferase activity resulting in de novo ceramide synthesis (59). Ceramide is enzymatically degraded by ceramidase to sphingosine (65,66). Sphingosine, through binding to ryanodine receptor, elicits a negative cardiac inotropic effect by inhibiting SR Ca^{2+} release (67), L-type Ca^{2+} channels, and $[Ca^{2+}]_i$ transients (68). Interestingly, ceramide itself does not depress cardiomyocyte contractile capacity (69,70) and $[Ca^{2+}]_i$ transients (68,70). These observations, in conjunction with data from this study, seem to suggest that cardiomyopathy under conditions of sustained dyslipidemia and lipid accumulation may be initiated and facilitated by both lipotoxic and nonlipotoxic mechanisms. In addition, ceramide may not be the ultimate culprit element responsible for compromised cardiomyocyte excitation-contraction coupling under conditions where lipotoxic cardiac dysfunction is present.

In summary, this study supports the notion that cardiomyocyte electrocardiographic alterations develop after high-fat and marginally copper-deficient diet intake (54,56). Our results showed that high dietary fat and marginal copper deficiency impaired cardiomyocyte contractile and $[Ca^{2+}]_i$ properties in the absence of overt lipotoxicity, nitrosative damage, and apoptosis. Our data suggest that certain $[Ca^{2+}]_i$ -regulating proteins such as PLB may be at fault for compromised $[Ca^{2+}]_i$ handling. It should be mentioned that our high-fat and/or marginally copper-deficient dietary feeding regimen in weanling animals used in this experimental setting did not induce any change in body FM, FM percentage, total body water volume, or obesity index (equivalent to BMI in humans), which would be normally expected in diet-induced human obesity. Therefore, special caution should be taken for proper interpretation of our experimental data in reference to human obesity.

Acknowledgments

The authors gratefully acknowledge Jim Lindlauf, Dr. Colin Combs, Jan Audette, Sharlene Rakoczy, Gwen Dahlen, Clint Hall, Barb Kueber, Denice Shafer, Kim Michelson, and Steve Dufault for skillful assistance in dietary feeding, animal experiments, and Western blot analysis. We also want to thank Dr. Katherine A. Sukalski from University of North Dakota School of Medicine and Dr. Eric O. Uthus from Human Nutrition Research Center (Grand Forks, ND) for critical comments on this manuscript. D.P.R. was a pre-doctoral fellowship recipient from the American Heart Association Northland Affiliate. This study was supported, in part, by grants from the

American Diabetes Association (7-0-RA-21) and the American Heart Association Northland Affiliate.

References

1. **Cooper R, Cutler J, Desvigne-Nickens P, et al.** Trends and disparities in coronary heart disease, stroke, and other cardiovascular diseases in the United States: findings of the national conference on cardiovascular disease prevention. *Circulation.* 2000;102:3137–47.
2. **Doggrell SA, Brown L.** Rat models of hypertension, cardiac hypertrophy and failure. *Cardiovasc Res.* 1998;39:89–105.
3. **Mensah GA, Mokdad AH, Ford E, et al.** Obesity, metabolic syndrome, and type 2 diabetes: emerging epidemics and their cardiovascular implications. *Cardiol Clin.* 2004;22:485–504.
4. **Ogden CL, Carroll MD, Curtin LR, McDowell MA, Tabak CJ, Flegal KM.** Prevalence of overweight and obesity in the United States, 1999–2004. *JAMA.* 2006;295:1549–55.
5. **de Divitiis O, Fazio S, Petitto M, Maddalena G, Contaldo F, Mancini M.** Obesity and cardiac function. *Circulation.* 1981;64:477–82.
6. **Zhou YT, Grayburn P, Karim A, et al.** Lipotoxic heart disease in obese rats: implications for human obesity. *Proc Natl Acad Sci U S A.* 2000;97:1784–9.
7. **Li SY, Yang X, Ceylan-Isik AF, Du M, Sreejayan N, Ren J.** Cardiac contractile dysfunction in Lep/Lep obesity is accompanied by NADPH oxidase activation, oxidative modification of sarco(endo)plasmic reticulum Ca2+-ATPase and myosin heavy chain isozyme switch. *Diabetologia.* 2006;49:1434–46.
8. **Ren J, Walsh MF, Jefferson L, et al.** Basal and ethanol-induced cardiac contractile response in lean and obese Zucker rat hearts. *J Biomed Sci.* 2000;7:390–400.
9. **Ren J, Sowers JR, Walsh MF, Brown RA.** Reduced contractile response to insulin and IGF-I in ventricular myocytes from genetically obese Zucker rats. *Am J Physiol Heart Circ Physiol.* 2000;279:H1708–14.
10. **Dobrian AD, Davies MJ, Schriver SD, Lauterio TJ, Prewitt RL.** Oxidative stress in a rat model of obesity-induced hypertension. *Hypertension.* 2001;37:554–60.
11. **Sowers JR.** Obesity and cardiovascular disease. *Clin Chem.* 1998;44:1821–5.
12. **Ren J, Walsh MF, Hamaty M, Sowers JR, Brown RA.** Augmentation of the inotropic response to insulin in diabetic rat hearts. *Life Sci.* 1999;65:369–80.
13. **Ren J, Walsh MF, Hamaty M, Sowers JR, Brown RA.** Altered inotropic response to IGF-I in diabetic rat heart: influence of intracellular Ca2+ and NO. *Am J Physiol.* 1998; 275:H823–30.
14. **Relling DP, Esberg LB, Fang CX, et al.** High-fat diet-induced juvenile obesity leads to cardiomyocyte dysfunction and upregulation of Foxo3a transcription factor independent of lipotoxicity and apoptosis. *J Hypertens.* 2006;24:549–61.
15. **Unger RH.** Lipotoxic diseases. *Annu Rev Med.* 2002;53:319–36.
16. **Hansen HS, Jensen B.** Essential function of linoleic acid esterified in acylglucosylceramide and acylceramide in maintaining the epidermal water permeability barrier. Evidence from feeding studies with oleate, linoleate, arachidonate, columbinate and alpha-linolenate. *Biochim Biophys Acta.* 1985;834:357–63.
17. **Ghayour-Mobarhan M, Taylor A, New SA, Lamb DJ, Ferns GA.** Determinants of serum copper, zinc and selenium in healthy subjects. *Ann Clin Biochem.* 2005;42:364–75.
18. **Klevay LM.** Heart failure improvement from a supplement containing copper. *Eur Heart J.* 2006;27:117–8.
19. **Klevay LM.** Cardiovascular disease from copper deficiency—a history. *J Nutr.* 2000;130(2S Suppl):489S–92S.
20. **Kennedy ML, Failla ML, Smith JC Jr.** Influence of genetic obesity on tissue concentrations of zinc, copper, manganese and iron in mice. *J Nutr.* 1986;116:1432–41.
21. **Donaldson DL, Smith CC, Koh E.** Effects of obesity and diabetes on tissue zinc and copper concentrations in the Zucker rat. *Nutr Res (NY).* 1987;7:393–9.
22. **Serfass RE, Park KE, Kaplan ML.** Developmental changes of selected minerals in Zucker rats. *Proc Soc Exp Biol Med.* 1988;189:229–39.
23. **Zargar AH, Shah NA, Masoodi SR, et al.** Copper, zinc, and magnesium levels in non-insulin dependent diabetes mellitus. *Postgrad Med J.* 1998;74:665–8.
24. **Saari JT, Schuschke DA.** Cardiovascular effects of dietary copper deficiency. *Biofactors.* 1999;10:359–75.
25. **Jenkins JE, Medeiros DM.** Diets containing corn oil, coconut oil and cholesterol alter ventricular hypertrophy, dilatation and function in hearts of rats fed copper-deficient diets. *J Nutr.* 1993;123:1150–60.
26. **Lear PM, Heller LJ, Prohaska JR.** Cardiac hypertrophy in copper-deficient rats is not attenuated by angiotensin II receptor antagonist L-158,809. *Proc Soc Exp Biol Med.* 1996;212: 284–92.
27. **Prohaska JR, Heller LJ.** Mechanical properties of the copper-deficient rat heart. *J Nutr.* 1982;112:2142–50.
28. **Kang YJ, Zhou ZX, Wu H, Wang GW, Saari JT, Klein JB.** Metallothionein inhibits myocardial apoptosis in copper-deficient mice: role of atrial natriuretic peptide. *Lab Invest.* 2000; 80:745–57.
29. **Fernandez-Lopez JA, Esteve M, Rafecas I, Remesar X, Alemany M.** Management of dietary essential metals (iron, copper, zinc, chromium and manganese) by Wistar and Zucker obese rats fed a self-selected high-energy diet. *Biometals.* 1994;7:117–29.
30. **Reeves PG, Nielsen FH, Fahey GC Jr.** AIN-93 purified diets for laboratory rodents: final report of the American Institute of Nutrition ad hoc writing committee on the reformulation of the AIN-76A rodent diet. *J Nutr.* 1993;123:1939–51.
31. **Reeves PG, Rossow KL, Lindlauf J.** Development and testing of the AIN-93 purified diets for rodents: results on growth, kidney calcification and bone mineralization in rats and mice. *J Nutr.* 1993;123:1923–31.
32. **Hall CB, Lukaski HC, Marchello MJ.** Estimation of rat body composition using tetrapolar bioelectrical impedance analysis. *Nutr Rep Int.* 1989;39:627–33.
33. **Fang CX, Dong F, Ren BH, Epstein PN, Ren J.** Metallothionein alleviates cardiac contractile dysfunction induced by insulin resistance: role of Akt phosphorylation, PTB1B, PPARgamma and c-Jun. *Diabetologia.* 2005;48:2412–21.
34. **Wold LE, Relling DP, Duan J, Norby FL, Ren J.** Abrogated leptin-induced cardiac contractile response in ventricular myocytes under spontaneous hypertension: role of Jak/STAT pathway. *Hypertension.* 2002;39:69–74.

35. **Dong F, Esberg LB, Roughead ZK, Ren J, Saari JT.** Increased contractility of cardiomyocytes from copper-deficient rats is associated with upregulation of cardiac IGF-I receptor. *Am J Physiol Heart Circ Physiol.* 2005;289:H78–84.
36. **Ren J, Porter JE, Wold LE, Aberle NS, Muralikrishnan D, Haselton JR.** Depressed contractile function and adrenergic responsiveness of cardiac myocytes in an experimental model of Parkinson disease, the MPTP-treated mouse. *Neurobiol Aging.* 2004;25:131–8.
37. **Bradford MM.** A rapid and sensitive method for the quantitation of microgram quantities of protein utilizing the principle of protein-dye binding. *Anal Biochem.* 1976;72:248–54.
38. **Dobrowsky RT, Kolesnick RN.** Analysis of sphingomyelin and ceramide levels and the enzymes regulating their metabolism in response to cell stress. *Methods Cell Biol.* 2001;66:135–65.
39. **Folch J, Lees M, Sloane Stanley GH.** A simple method for the isolation and purification of total lipides from animal tissues. *J Biol Chem.* 1957;226:497–509.
40. **Brockerhoff H.** Determination of the positional distribution of fatty acids in glycerolipids. *Methods Enzymol.* 1975;35:315–25.
41. **Prows DR, Murphy EJ, Moncecchi D, Schroeder F.** Intestinal fatty acid-binding protein expression stimulates fibroblast fatty acid esterification. *Chem Phys Lipids.* 1996;84:47–56.
42. **Gavrieli Y, Sherman Y, Ben Sasson SA.** Identification of programmed cell death in situ via specific labeling of nuclear DNA fragmentation. *J Cell Biol.* 1992;119:493–501.
43. **Ren J, Wold LE, Natavio M, Ren BH, Hannigan JH, Brown RA.** Influence of prenatal alcohol exposure on myocardial contractile function in adult rat hearts: role of intracellular calcium and apoptosis. *Alcohol Alcohol.* 2002;37:30–7.
44. **Chirico S.** High-performance liquid chromatography-based thiobarbituric acid tests. *Methods Enzymol.* 1994;233:314–8.
45. **Yarian CS, Rebrin I, Sohal RS.** Aconitase and ATP synthase are targets of malondialdehyde modification and undergo an age-related decrease in activity in mouse heart mitochondria. *Biochem Biophys Res Commun.* 2005;330:151–6.
46. **Davies NT, Lawrence CB, Mills CF.** Studies on the effects of copper deficiency on rat liver mitochondria. II. Effects on oxidative phosphorylation. *Biochim Biophys Acta.* 1985;809:362–8.
47. **Johnson WT, Demars LC.** Increased heme oxygenase-1 expression during copper deficiency in rats results from increased mitochondrial generation of hydrogen peroxide. *J Nutr.* 2004;134:1328–33.
48. **Sarti C, Gallagher J.** The metabolic syndrome: prevalence, CHD risk, and treatment. *J Diabetes Complications.* 2006;20:121–32.
49. **Dobrian AD, Davies MJ, Prewitt RL, Lauterio TJ.** Development of hypertension in a rat model of diet-induced obesity. *Hypertension.* 2000;35:1009–15.
50. **Norby FL, Wold LE, Duan J, Hintz KK, Ren J.** IGF-I attenuates diabetes-induced cardiac contractile dysfunction in ventricular myocytes. *Am J Physiol Endocrinol Metab.* 2002;283:E658–66.
51. **Roberts CK, Vaziri ND, Wang XQ, Barnard RJ.** Enhanced NO inactivation and hypertension induced by a high-fat, refined-carbohydrate diet. *Hypertension.* 2000;36:423–9.
52. **Bjorbaek C, Uotani S, da Silva B, Flier JS.** Divergent signaling capacities of the long and short isoforms of the leptin receptor. *J Biol Chem.* 1997;272:32686–95.
53. **Saari JT.** Copper deficiency and cardiovascular disease: role of peroxidation, glycation, and nitration. *Can J Physiol Pharmacol.* 2000;78:848–55.
54. **Mao S, Medeiros DM, Hamlin RL.** Marginal copper and high fat diet produce alterations in electrocardiograms and cardiac ultrastructure in male rats. *Nutrition.* 1999;15:890–8.
55. **Saari JT.** Renal copper as an index of copper status in marginal deficiency. *Biol Trace Elem Res.* 2002;86:237–47.
56. **Wildman RE, Hopkins R, Failla ML, Medeiros DM.** Marginal copper-restricted diets produce altered cardiac ultrastructure in the rat. *Proc Soc Exp Biol Med.* 1995;210:43–9.
57. **Sowers JR.** Obesity as a cardiovascular risk factor. *Am J Med.* 2003;115(Suppl 8A):37S–41S.
58. **Ren J, Ceylan-Isik AF.** Diabetic cardiomyopathy: do women differ from men? *Endocrine.* 2004;25:73–83.
59. **Shimabukuro M, Higa M, Zhou YT, Wang MY, Newgard CB, Unger RH.** Lipoapoptosis in beta-cells of obese prediabetic fa/fa rats. Role of serine palmitoyltransferase overexpression. *J Biol Chem.* 1998;273:32487–90.
60. **Houser SR, Piacentino V III, Weisser J.** Abnormalities of calcium cycling in the hypertrophied and failing heart. *J Mol Cell Cardiol.* 2000;32:1595–607.
61. **Duan J, Zhang HY, Adkins SD, et al.** Impaired cardiac function and IGF-I response in myocytes from calmodulin-diabetic mice: role of Akt and RhoA. *Am J Physiol Endocrinol Metab.* 2003;284:E366–76.
62. **Huang B, Wang S, Qin D, Boutjdir M, El Sherif N.** Diminished basal phosphorylation level of phospholamban in the postinfarction remodeled rat ventricle: role of beta-adrenergic pathway, G(i) protein, phosphodiesterase, and phosphatases. *Circ Res.* 1999;85:848–55.
63. **Lin WH, Chen MD, Wang CC, Lin PY.** Dietary copper supplementation increases the catecholamine levels in genetically obese (*ob/ob*) mice. *Biol Trace Elem Res.* 1995;50:243–7.
64. **Ghibaudi L, Cook J, Farley C, van Heek M, Hwa JJ.** Fat intake affects adiposity, comorbidity factors, and energy metabolism of Sprague-Dawley rats. *Obes Res.* 2002;10:956–63.
65. **Zhang DX, Fryer RM, Hsu AK, et al.** Production and metabolism of ceramide in normal and ischemic-reperfused myocardium of rats. *Basic Res Cardiol.* 2001;96:267–74.
66. **Franzen R, Pfeilschifter J, Huwiler A.** Nitric oxide induces neutral ceramidase degradation by the ubiquitin/proteasome complex in renal mesangial cell cultures. *FEBS Lett.* 2002;532:441–4.
67. **Sabbadini RA, Betto R, Teresi A, Fachechi-Cassano G, Salviati G.** The effects of sphingosine on sarcoplasmic reticulum membrane calcium release. *J Biol Chem.* 1992;267:15475–84.
68. **McDonough PM, Yasui K, Betto R, et al.** Control of cardiac Ca^{2+} levels. Inhibitory actions of sphingosine on Ca2+ transients and L-type Ca2+ channel conductance. *Circ Res.* 1994;75:981–9.
69. **Oral H, Dorn GW, Mann DL.** Sphingosine mediates the immediate negative inotropic effects of tumor necrosis factor-alpha in the adult mammalian cardiac myocyte. *J Biol Chem.* 1997;272:4836–42.
70. **Relling DP, Hintz KK, Ren J.** Acute exposure of ceramide enhances cardiac contractile function in isolated ventricular myocytes. *Br J Pharmacol.* 2003;140:1163–8.